RESEARCH　　　　　　　　　　　　　　　　　　　　　　　　　　　**Open Access**

Induction of cellulase production by Sr^{2+} in *Trichoderma reesei* via calcium signaling transduction

Ni Li, Yi Zeng, Yumeng Chen, Yaling Shen and Wei Wang[*]

Abstract

Trichoderma reesei RUT-C30 is a well-known high-yielding cellulase-producing fungal strain that converts lignocellulose into cellulosic sugar for resource regeneration. Calcium is a ubiquitous secondary messenger that regulates growth and cellulase production in *T. reesei*. We serendipitously found that adding Sr^{2+} to the medium significantly increased cellulase activity in the *T. reesei* RUT-C30 strain and upregulated the expression of cellulase-related genes. Further studies showed that Sr^{2+} supplementation increased the cytosolic calcium concentration and activated the calcium-responsive signal transduction pathway of Ca^{2+}–calcineurin-responsive zinc finger transcription factor 1 (CRZ1). Using the plasma membrane Ca^{2+} channel blocker, $LaCl_3$, we demonstrated that Sr^{2+} induces cellulase production via the calcium signaling pathway. Supplementation with the corresponding concentrations of Sr^{2+} also inhibited colony growth. Sr^{2+} supplementation led to an increase in intracellular reactive oxygen species (ROS) and upregulated the transcriptional levels of intracellular superoxide dismutase (*sod1*) and catalase (*cat1*). We further demonstrated that ROS content was detrimental to cellulase production, which was alleviated by the ROS scavenger *N*-acetyl cysteine (NAC). This study demonstrated for the first time that Sr^{2+} supplementation stimulates cellulase production and upregulates cellulase genes via the calcium signaling transduction pathway. Sr^{2+} leads to an increase in intracellular ROS, which is detrimental to cellulase production and can be alleviated by the ROS scavenger NAC. Our results provide insights into the mechanistic study of cellulase synthesis and the discovery of novel inducers of cellulase.

Keywords: *Trichoderma reesei*, Sr^{2+}, Cellulase, ROS, Calcium signaling, Signal transduction

---

*Correspondence: wadexp@ecust.edu.cn

The State Key Laboratory of Bioreactor Engineering, New World Institute of Biotechnology, East China University of Science and Technology, Shanghai 200237, China

Li *et al. Bioresources and Bioprocessing*   (2022) 9:96

Page 2 of 12

Graphical Abstract
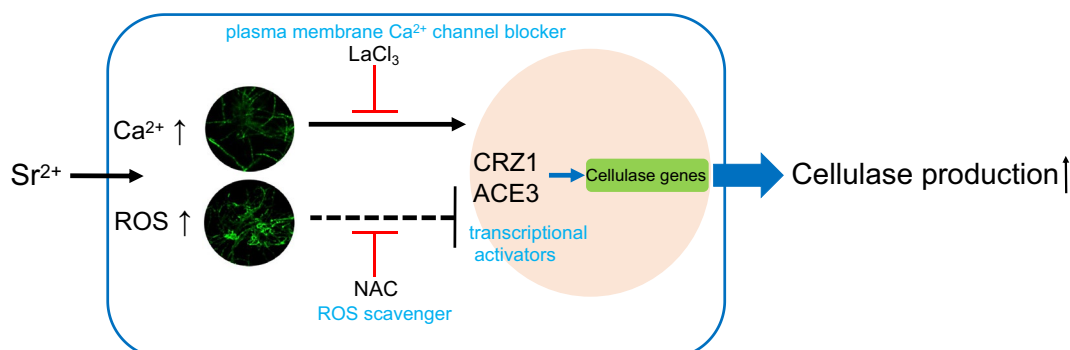
Introduction

Lignocellulose is a well-known renewable biomass energy source that can be degraded to bioethanol (Baldrian and Valášková 2008; Somerville et al. 2010). The economic and practical degradation of cellulose has been widely recognized and accepted (Li et al. 2018). Cellulose degradation is dependent on *Trichoderma reesei*, a strain that efficiently produces cellulase and hemicellulase (Fischer et al. 2021; Li et al. 2016, 2021; Martzy et al. 2021; Yan et al. 2021). *Trichoderma reesei* can produce large amounts of cellulases and hemicellulases using inducible carbon sources (such as Avicel). In contrast, negligible amounts of cellulases and hemicellulases are produced using fast-utilizing carbon sources (such as glucose) (Antoniêto et al. 2016). The production of cellulases is an extremely complex process regulated by many factors, such as transcription factors (Xin et al. 2010) and the second messenger Ca^{2+} (Chen et al. 2019).

Cellulase synthesis in *T. reesei* is regulated by several transcription factors (Zhang et al. 2018). Among these factors, xylanase regulator 1 (XYR1) is involved in activation of the expression of cellulases and hemicellulases (Carle-Urioste et al. 1997; Furukawa et al. 2009; Zeilinger et al. 1996), as well as the regulation of ᴅ-xylose metabolism (Stricker et al. 2006), which is considered as a key transactivator (Cao et al. 2019). Deletion of *xyr1* results in a substantial reduction in cellulase and hemicellulase production (Stricker et al. 2006). ACE3, another crucial transcriptional activator, is essential for cellulase and xylanase production (Häkkinen et al. 2014). Deletion of *ace3* is fatal for cellulase gene expression, whereas this deletion slightly reduces the expression of hemicellulases (Luo et al. 2020) and xylanase (Zhang et al. 2019).

Ca^{2+} signaling is a well-known secondary signaling pathway that broadly regulates primary and secondary metabolism in microorganisms (Roy et al. 2021).

The intracellular calcium signaling components include free Ca^{2+}, calmodulin (CaM), calcineurin (CnA), and calcineurin-responsive zinc finger transcription factor 1 (Crz1) (Bootman et al. 2002). Increases in cytosolic Ca^{2+} levels lead to the activation of Crz1 via Ca^{2+}/CaM/CnA, which activates downstream genes with different functions by binding to their promoter regions (Martins-Santana et al. 2020). Chen et al. (2016) reported that the cytosolic Ca^{2+} concentration activates the binding of the transcription factor Crz1 to the cellulase gene *cbh1* and main transcriptional activator of cellulase genes *xyr1*, thereby upregulating cellulase gene expression. Notably, Chen et al. (2018) demonstrated that Mn^{2+} induces a cytosolic Ca^{2+} burst to enhance the expression of cellulase genes through the Mn^{2+}/Ca^{2+} exchanger in *T. reesei*. In *Penicillium brevicompactum*, addition of Ca^{2+} increases the production of the secondary metabolite mycophenolic acid (Chen et al. 2021a).

Reactive oxygen species (ROS) are chemically reactive chemicals that contain oxygen and are considered as harmful by-products of aerobic metabolism (Ren et al. 2017). ROS play a critical role in the development of many filamentous fungi, including *Aspergillus nidulans* (Mendoza-Martínez et al. 2017), *Podospora anserina* (Malagnac et al. 2004), and *Neurospora crassa* (Takemoto et al. 2007). Chen et al. (2022) demonstrated that a higher concentration of Mn^{2+} increased ROS production, ultimately leading to increased mycophenolic acid production in *P. brevicompactum*. Liu et al. (2018) observed that the ROS producer H_2O_2 and ROS scavenger *N*-acetyl cysteine (NAC) altered intracellular ROS levels in *Ganoderma lucidum*, which is an efficient approach for enhancing the production of ganoderic acid.

Ca^{2+} can promote the transcription of cellulase genes in the hypercellulolytic *T. reesei* strain RUT-C30. Therefore, we investigated whether other ions of group IIA

Li *et al. Bioresources and Bioprocessing*   (2022) 9:96

Page 3 of 12

metals can also increase cellulase production. High Mg^{2+} concentrations significantly inhibit growth (Groisman et al. 2013), which was not considered in this study. Furthermore, a previous study on Ca^{2+} was conducted in *T. reesei* RUT-C30. Therefore, in the current study, the effect of Sr^{2+} on cellulase production was investigated using RUT-C30. The effects of Sr^{2+} on mycelial growth and cellulase production were measured, and the transcript levels of *crz1* and intracellular Ca^{2+} levels were evaluated to determine the role of calcium signaling in response to Sr^{2+}. This study provides new perspectives for improving cellulase production and insights into the mechanism of cellulase regulation in *T. reesei*.

Materials and methods
Strains and growth conditions
Trichoderma reesei RUT-C30 (ATCC 56765) and QM6a (ATCC 13631) were used for the experiments. All *T. reesei* strains were cultured on potato dextrose agar (PDA) plates at 28 °C in the dark. Fresh conidia were washed with PDA plates and inoculated. MA medium (Zhang et al. 2019) was used for the general fungal culture. Minimal medium (MM; $(NH_4)_2SO_4$ 5 g/L; KH_2PO_4 15 g/L; urea 0.3 g/L; $MgSO_4$ 0.6 g/L; $CaCl_2$ 0.6 g/L; $FeSO_4 \cdot 7H_2O$ 5 mg/L; $CoCl_2 \cdot 6H_2O$ 2 mg/L; $MnSO_4 \cdot H_2O$ 1.6 mg/L; $ZnSO_4 \cdot 7H_2O$ 1.4 mg/L; pH 5.5) (Chen et al. 2018) with 2% (w/v) glucose or 1% (w/v) Avicel was used to assess the effect of Sr^{2+} on hyphal growth and cellulase production. Transfer experiments were performed to study the effects of Sr^{2+} on cellulase production. The conidia were first cultured in 100 mL MA medium containing 2% glucose at 28 °C for 36 h to form mycelia. Mycelia (1 mL) were collected by centrifugation, washed with MM without a carbon source, and transferred into 50 mL of fresh MM containing 1% (w/v) Avicel (PH-101; Sigma-Aldrich, St. Louis, MO, USA) with the addition of $SrCl_2$ to final concentrations of 0–120 mM.

Enzyme activity analysis and fungal growth
The culture (1 mL) was collected and centrifuged at $14,000 \times g$ at 4 °C for 5 min. The resulting supernatant was used to determine cellulase activity. *p*NPCase, CMCase, FPase, and xylanase activities were measured as previously reported (Zhang et al. 2016; Liu et al. 2019). The Detergent Compatible Bradford Protein Assay Kit (Beyotime, Shanghai, China) was used to determine protein concentrations. Biomass was measured indirectly using the intracellular protein method (Bischof et al. 2013) with some modifications. Three parallel samples (1 mL each) was collected, and the mycelia were collected by filtration, lysed with 1 M NaOH for 2 h, and centrifuged to obtain the intracellular proteins. The BCA Protein Concentration Assay Kit (Beyotime, Shanghai, China) was used to determine the total protein concentration. The biomass dry weight was calculated as 0.32 g intracellular protein per gram of dry cell weight (Chen et al. 2018).

For fungal growth experiments, fresh conidia were diluted to 2.5×10^6/mL with sterile water, inoculated an equal volume of conidia fluid (2 μL) into the center of MM plates, and incubated at 28 °C in the dark for 4 days.

RNA extraction and RT-qPCR
RNA isolation and reverse transcription quantitative polymerase chain reaction (RT-qPCR) analyses were performed as described by Zhang et al. (2018) with some modifications. Briefly, total RNA from mycelia was extracted using the FastRNA Pro Red Kit (MPbio, Irvine, CA, USA) according to the manufacturer's instructions. cDNA was synthesized from total RNA using the Trans-Script Uni All-in-One First-Strand cDNA Synthesis SuperMix for qPCR (TransGen Biotech, Beijing, China). For RT-qPCR, the transcriptional levels of *cbh1* (encoding cellobiohydrolase I), *egl1* (encoding endoglucanase I), *xyr1* (encoding the main factor XYR1), *ace3* (encoding the main factor ACE3), *crz1* (calcineurin-responsive zinc finger transcription factor 1, Trire2:36391), *sod1* (copper/zinc superoxide dismutase, Trire2:123029), and *cat1* (catalase, Trire2:70600) were analyzed using PerfectStart™ Green qPCR SuperMix (TransGen Biotech). The $2^{-\Delta\Delta Ct}$ method was used for calculations (Livak and Schmittgen 2001). The *sar1* gene was used as an internal reference to normalize the data. The primers used for RT-qPCR are described in Additional file 2: Table S1.

Labeling and detection of cytosolic Ca^{2+} and ROS
Cytosolic Ca^{2+} and ROS levels were assessed according to the manufacturer's instructions, with some modifications. For fluorescent detection of Ca^{2+} and ROS, the mycelia were incubated with the fluorescent probe Fluo-4 AM/DCHF-DA (Beyotime, Shanghai, China) at 28 °C for 30 min. The mycelia were washed three times with phosphate-buffered saline (PBS) (pH 5.0) to remove excess fluorophores and avoid excessive background noise. Images of the DCF- and Fluo-4 AM-labeled mycelia were visualized using an S Plan Fluor ELWD 20×, 0.5 numerical aperture (NA) objective and a digital sight camera on an Eclipse Ti inverted microscope system (Ti-E; Nikon, Tokyo, Japan), comprising a FITC filter (420–490 nm band-pass excitation filter and an emission filter of 535 nm). The average fluorescence intensities were analyzed using ImageJ software (National Institutes of Health, Bethesda, MD, USA).

Li *et al. Bioresources and Bioprocessing*   (2022) 9:96

Page 4 of 12

Chemical treatments

To evaluate the effect of Sr^{2+} on cellulase production, different concentrations of $SrCl_2$ were added immediately after transferring the mycelia to fresh MM. To evaluate the roles of cytosolic Ca^{2+} and ROS under Sr^{2+} stress, the mycelia were treated with the ROS scavenger NAC, hydrogen peroxide (H_2O_2), and plasma membrane Ca^{2+} channel blocker ($LaCl_3$). NAC was added immediately after the mycelia were transferred to fresh MM. $LaCl_3$ and H_2O_2 were added at 24 h after the mycelia were transferred to fresh MM.

Statistical analysis

All experimental data were obtained with at least three parallel samples with similar or identical results. Error values represent the standard deviation (SD) from the mean of three replicates. Student's *t*-test was used to compare two samples to detect statistical significance. Duncan's multiple-range test was used for multiple comparisons. Differences were considered as significant at $p < 0.05$.

Results

Effects of Sr^{2+} on *T. reesei* growth

To investigate the effect of Sr^{2+} on colony growth, different concentrations of Sr^{2+} (0–120 mM) were added to solid MM containing 20 g/L glucose as the sole carbon source. An equal amount of fresh RUT-C30 conidia was spotted onto poured plates. The growth status of mycelia after Sr^{2+} supplementation is shown in Fig. 1a. The *T. reesei* strains grew more slowly as the Sr^{2+} concentration was increased. As shown in Fig. 1b, hyphal growth significantly differed between the 50 mM Sr^{2+} and no Sr^{2+} supplementation groups. Treatment with 70 and 100 mM Sr^{2+} caused a 31% and 35.2% reduction in colony diameter, respectively, compared to that of untreated strains. When the Sr^{2+} concentration was increased to 120 mM, the treated strains exhibited the most severe reduction in colony diameter (approximately 46.9%). This result was consistent with the biomass production data for MM liquid culture with 1% (w/v) Avicel as the sole carbon source (Fig. 1c). These results indicate that supplementation with large amounts of Sr^{2+} inhibited the growth of *T. reesei* strains under both glucose and Avicel carbon sources.
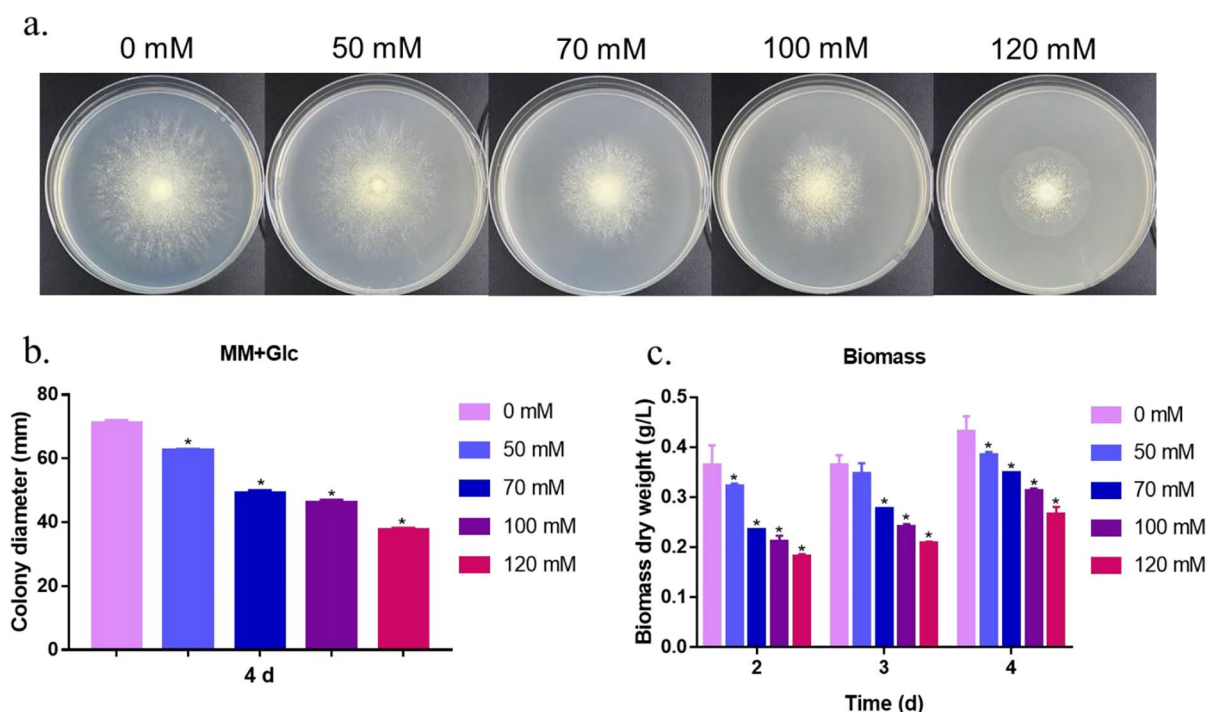

Fig. 1 Effect of different concentrations of Sr^{2+} on hyphal growth in *T. reesei* RUT-C30 strain. **a** Hyphal growth of RUT-C30 strain on MM plates. The MM culture was supplemented with Sr^{2+} at a final concentration of 0–120 mM. **b** Colony diameter under different concentrations of Sr^{2+}. **c** Biomass dry weight in MM liquid culture of RUT-C30 strain. The final values are presented as the mean ± standard deviation (SD) of three independent experimental results. Asterisks indicate significant differences compared to the control ($p < 0.05$, according to Student's *t*-test). MM, minimal medium
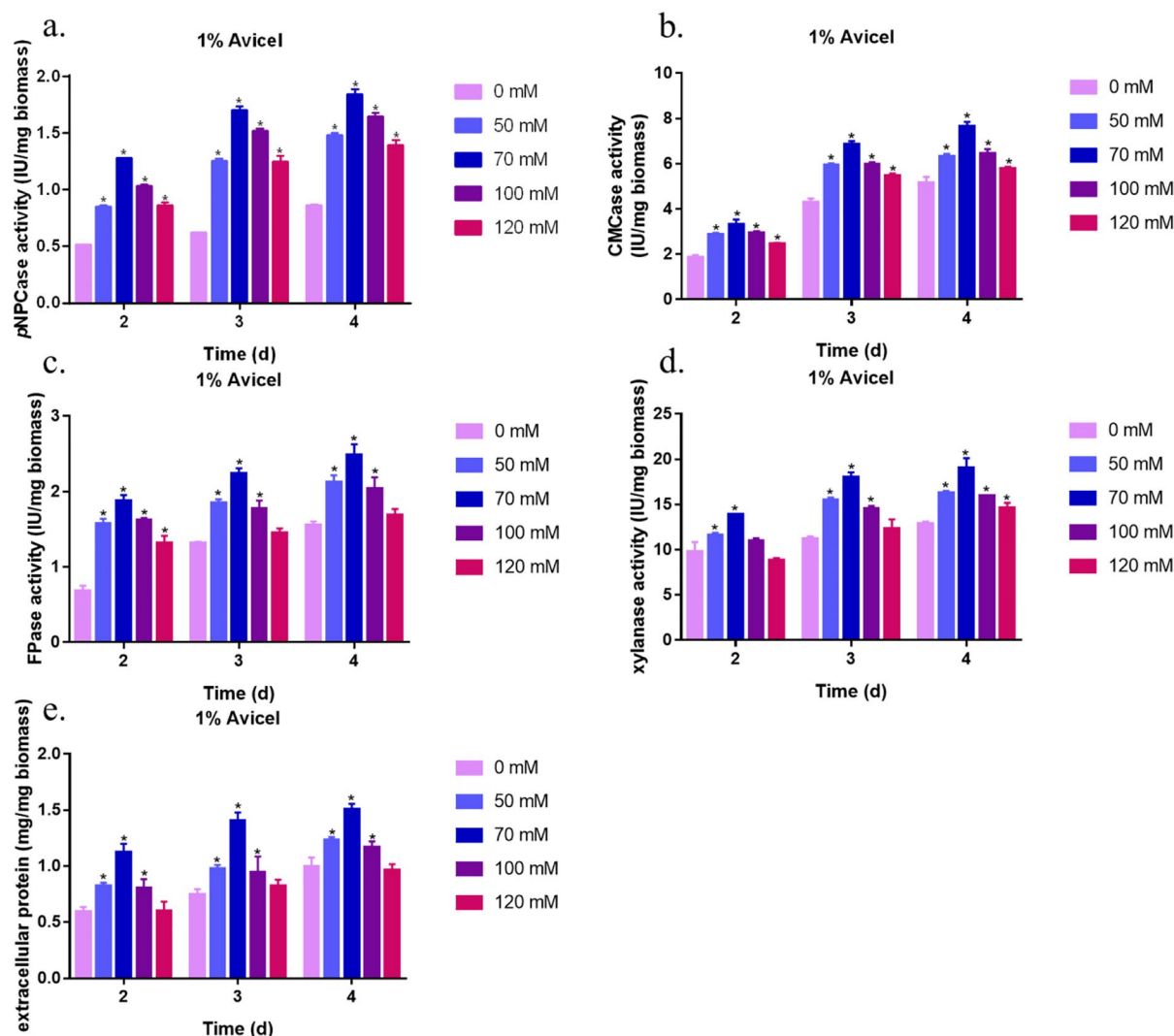
Li *et al. Bioresources and Bioprocessing*　　(2022) 9:96

Page 5 of 12

Fig. 2 Effect of Sr^{2+} on cellulase production in RUT-C30 strain. *p*NPCase activity (**a**), CMCase activity (**b**), FPase activity (**c**), xylanase activity (**d**), and total protein concentrations (**e**) of the RUT-C30 strain were examined after culture in MM for 2, 3, or 4 days containing different concentrations of Sr^{2+} (0–120 mM). The final values are presented as the mean ± standard deviation (SD) of three independent experimental results. Asterisks indicate significant differences compared to the control ($p < 0.05$, according to Student's *t*-test). MM, minimal medium

Cellulase production increased under Sr^{2+} pressure in *T. reesei*

To evaluate the effect of Sr^{2+} on cellulase production, the same amount of RUT-C30 mycelia was transferred into liquid MM with 1% (w/v) Avicel as the carbon source and different concentrations of Sr^{2+} (0–120 mM). As shown in Fig. 2a–e, addition of different concentrations of Sr^{2+} significantly improved cellulase activity and total protein secretion. Addition of 70 mM Sr^{2+} resulted in the largest improvement and significantly increased the *p*NPCase, CMCase, FPase, and xylanase activities, as well as the total protein concentration by 176%, 59.6%, 69.6%, 60%, and 87.2%, respectively, compared to that in the control

(without Sr^{2+}) on day 3 of cultivation. These results indicate that addition of 50–120 mM Sr^{2+} significantly improved the cellulase yield. The optimal concentration of Sr^{2+} for enhancing cellulase production was 70 mM in RUT-C30, which was used in subsequent analyses.

To further investigate the effect of Sr^{2+} on cellulase synthesis, the expression levels of two vital cellulase genes (*cbh1* and *egl1*) and essential cellulase transcription activators *xyr1* and *ace3* were detected using RT-qPCR, as shown in Fig. 3. The transcription levels of *cbh1* and *egl1* increased by 546% and 520%, respectively, at 48 h, which was consistent with the upregulation of enzyme activities after addition of 70 mM Sr^{2+} (Fig. 2a–e). Addition of Sr^{2+}
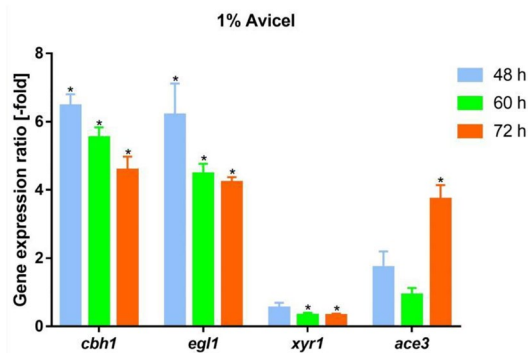
Li *et al. Bioresources and Bioprocessing*   (2022) 9:96

Page 6 of 12

Fig. 3 Effect of Sr^{2+} on cellulase-related gene transcription levels in RUT-C30 strain. Gene expression ratios [-fold] of *cbh1*, *egl1*, *xyr1*, and *ace3* in RUT-C30 treated with 70 mM Sr^{2+} relative to RUT-C30 without treatment on 1% Avicel for 48, 60, or 72 h. Gene expression ratios [-fold] were normalized to the corresponding gene expression at the same timepoint in the control (without Sr^{2+}). The final values are represented as the mean ± standard deviation (SD) of three independent experimental results. Asterisks indicate significant differences, representing gene expression ratio greater than twofold or less than 0.5-fold between the treated samples and those without Sr^{2+} treatment

upregulated the expression of cellulase activator *ace3* by approximately 72.3% at 48 h (Fig. 3). At 72 h, the expression level of *ace3* increased to 272% compared to that in the control. These results indicate that Sr^{2+} supplementation significantly increased the transcription levels of cellulase genes and the essential cellulase transcription activator *ace3*. However, addition of Sr^{2+} led to downregulation of *xyr1* expression (approximately 46%) at 48 h (Fig. 3).

Cytosolic Ca^{2+} accumulation in *T. reesei* was induced by high Sr^{2+} concentrations

Cytosolic concentrations of Ca^{2+} were detected using the fluorescent probe Fluo-4 AM, which emits green fluorescence after crossing the cell membrane and binding to cytosolic Ca^{2+} (Chen et al. 2021b). The fluorescence intensity represents the relative amount of free intracellular Ca^{2+}. As shown in Fig. 4a, following addition of 70 mM Sr^{2+}, the green fluorescence intensity in RUT-C30 cells was stronger than that in the control (without Sr^{2+} treatment). Analysis using ImageJ software showed that the fluorescence intensity of the experimental group
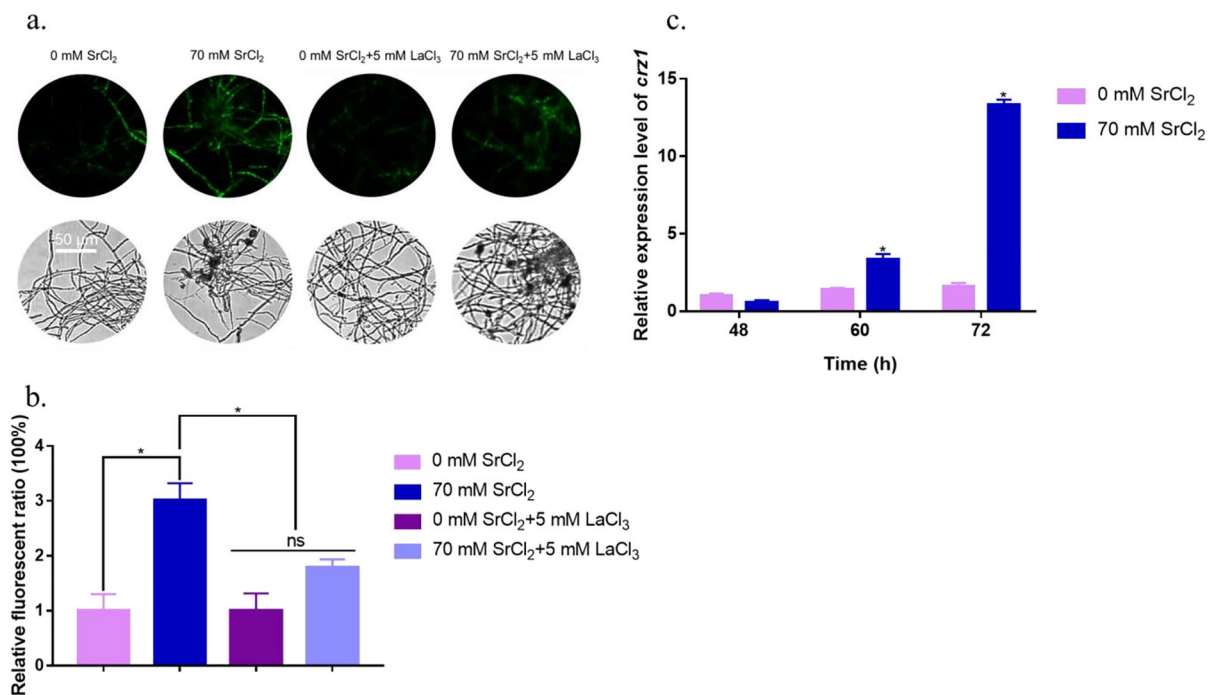

Fig. 4 Cytosolic Ca^{2+} levels increase after Sr^{2+} addition. **a** Cytosolic Ca^{2+} levels were detected using the specific fluorescent probe Fluo-4 AM. *Trichoderma reesei* RUT-C30 strain was cultured in MM for 2 days with or without supplementation of the Ca^{2+} channel inhibitor LaCl$_3$ and 0 or 70 mM Sr^{2+}. To treat hyphae, 4 μM Fluo-4 AM was used. For detection, automatic inverted fluorescence microscopy was used to monitor the fluorescence intensity. Stronger green fluorescence indicated a higher intracellular Ca^{2+} content. **b** Comparative fluorescence ratios demonstrating the effects of LaCl$_3$ on the cytosolic Ca^{2+} burst induced by Sr^{2+}. The *y*-axis represents the Ca^{2+} fluorescence ratio measured by CLSM, and the *x*-axis represents different treatments with Sr^{2+} and LaCl$_3$. **c** Transcriptional levels of *crz1* after treatment with 0 or 70 mM Sr^{2+} for 48, 60, or 72 h were also detected. The final values are presented as the mean ± standard deviation (SD) from three independent experimental results. Asterisks indicate significant differences compared to the strain without Sr^{2+} treatment ($p < 0.05$, according to Student's *t*-test). DIC, differential interference contrast; MM, minimal medium

Li *et al. Bioresources and Bioprocessing*　　　(2022) 9:96

Page 7 of 12

increased by twofold after addition of Sr^{2+} (Fig. 4b), suggesting that the cytosolic Ca^{2+} content increased after Sr^{2+} treatment.

Increased concentrations of the second messenger Ca^{2+} in the cytosol lead to a response in the downstream calcium pathway (Li et al. 2019; Liu et al. 2019). Crz1, a critical activator of the calcium signal transduction terminal, plays an essential role in calcium signal transduction pathways (Chen et al. 2016; Martins-Santana et al. 2020). The transcription level of the transcriptional regulator *crz1* detected using RT-qPCR was upregulated after Sr^{2+} induction (Fig. 4c).

A plasma membrane Ca^{2+} channel blocker, $LaCl_3$ (Zhang et al. 2022), which prevents the influx of extracellular calcium ions, was used to examine the effect of Sr^{2+} on the cytosolic Ca^{2+} burst. As illustrated in Fig. 4a, b, the significant increase in intracellular Ca^{2+} induced by Sr^{2+} was markedly weakened after supplementation with $LaCl_3$. At 5 mM $LaCl_3$, the fluorescence intensity of the mycelia decreased by 40.6% compared with that in the absence of $LaCl_3$. However, $LaCl_3$ supplementation only negligibly reduced the fluorescence intensity compared with that in the control without Sr^{2+} (Fig. 4b).

These results indicate that Sr^{2+} induces a cytosolic calcium burst and results in calcium signal transduction, and that adding a plasma membrane Ca^{2+} channel blocker can block the Sr^{2+}-induced calcium burst (Fig. 4b).

Sr^{2+} induced cytosolic Ca^{2+} burst and substantially increased cellulase production

$LaCl_3$ (5 mM) can block the Sr^{2+}-induced calcium burst (Fig. 4b). To explore whether blocking the cytosolic Ca^{2+} burst attenuates Sr^{2+}-induced cellulase overexpression, the activities of pNPCase (Fig. 5a) and CMCase (Fig. 5b) and the transcriptional levels of the vital cellulase genes *cbh1* (Fig. 5c) and *egl1* (Fig. 5d) were measured.

Under 5 mM $LaCl_3$ treatment, 70 mM Sr^{2+} did not induce cellulase overproduction in *T. reesei*. The pNPCase and CMCase activities decreased by 1.85- to 2.97-fold and 1.17- to 2.22-fold, respectively, when $LaCl_3$ was added compared to the sample without $LaCl_3$ addition at 2–4 days of cultivation (Fig. 5a, b). The transcript levels of *cbh1* and *egl1* were consistent with the cellulase activity data. After $LaCl_3$ addition, the expression levels of *cbh1* and *egl1* decreased to 20–30%
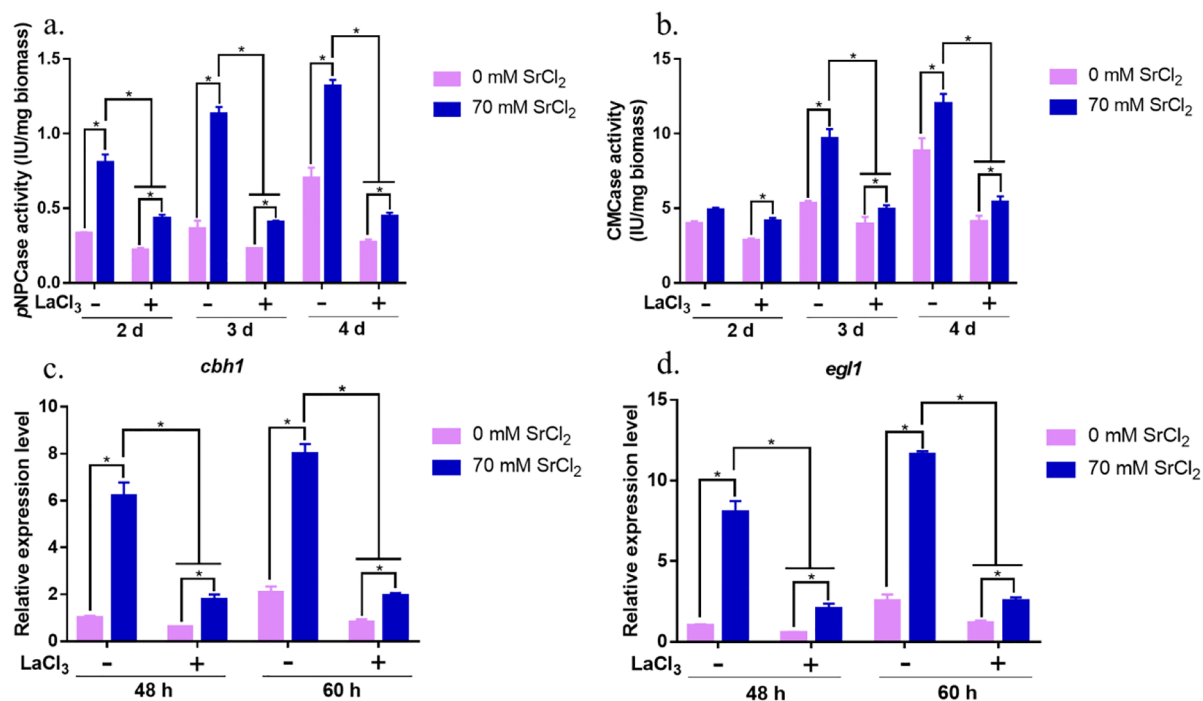

Fig. 5 Effect of $LaCl_3$ on cellulase production after Sr^{2+} treatment. pNPCase (**a**) and CMCase (**b**) activity were measured in the RUT-C30 strain after treatment with Sr^{2+} or $LaCl_3$. The transcriptional levels of *cbh1* (**c**) and *egl1* (**d**) were determined after culturing the RUT-C30 strain in medium supplemented with 0 or 70 mM Sr^{2+} and with (+) or without (−) 5 mM $LaCl_3$. The final values are represented as the mean ± standard deviation (SD) of three independent experimental results. Asterisks indicate significant differences compared to the strain without Sr^{2+} treatment ($p < 0.05$, according to Student's *t*-test)

(Fig. 5c, d). Sr^{2+}-induced cellulase overexpression was significantly attenuated by $LaCl_3$ treatment.

These results indicate that blocking the burst of cytosolic Ca^{2+} by $LaCl_3$ substantially reduced and even eliminated the induction of cellulase production by 70 mM Sr^{2+}. The cytosolic Ca^{2+} and calcium signaling pathways participate in Sr^{2+}-induced cellulase overproduction in *T. reesei*. High cellulase expression induced by Sr^{2+} was due to a Ca^{2+} burst in the cytoplasm.

Cytosolic ROS levels are significantly upregulated

The ROS content in mycelia exposed to Sr^{2+} was detected using the fluorescent probe dichlorodihydrofluorescein diacetate (DCFH-DA) (Gao et al. 2018). As shown in Fig. 6a, the green fluorescence intensity of the strain exposed to 70 mM Sr^{2+} was enhanced compared to that of the control (without Sr^{2+} supplementation), indicating that Sr^{2+}-induced stress increased cytosolic ROS levels. To further evaluate the influence of Sr^{2+} on the cytosolic ROS content, the transcript levels of two major antioxidant enzymes, catalase (CAT) and superoxide dismutase (SOD), were detected using RT-qPCR (Fig. 6b). After addition of 70 mM Sr^{2+}, the expression of *sod1* increased by approximately 78–150% at 48–60 h. The transcript levels of *cat1* increased by 165–487% at 60–72 h, indicating that the strain was under high ROS pressure.

NAC and H_2O_2 were used to alter the intracellular ROS content. As shown in Fig. 7a, b, adding 4 mM H_2O_2 reduced the levels of *p*NPCase and CMCase activity (approximately 33.1% and 16.8%, respectively). When the *T. reesei* strains were treated with 3 mM NAC, *p*NPCase and CMCase activities were markedly increased compared to those without NAC treatment (Fig. 7a–d). Under 70 mM Sr^{2+} treatment, *p*NPCase and CMCase activities also slightly increased in the presence of 3 mM NAC (approximately 11.5% and 8.4%, respectively). As shown in Fig. 7e, biomass production was measured following different chemical treatments. Addition of NAC slightly increased biomass production (approximately 11.9%), whereas treatment with H_2O_2 decreased biomass production (approximately 18.6%). Combined treatment with Sr^{2+} and H_2O_2 resulted in a large decrease in biomass (approximately 31.7%).

These results indicate that supplementation with 70 mM Sr^{2+} markedly increased ROS levels during *T. reesei* cultivation. Addition of the ROS scavenger NAC also decreased the ROS levels produced by Sr^{2+} and increased cellulase activity.
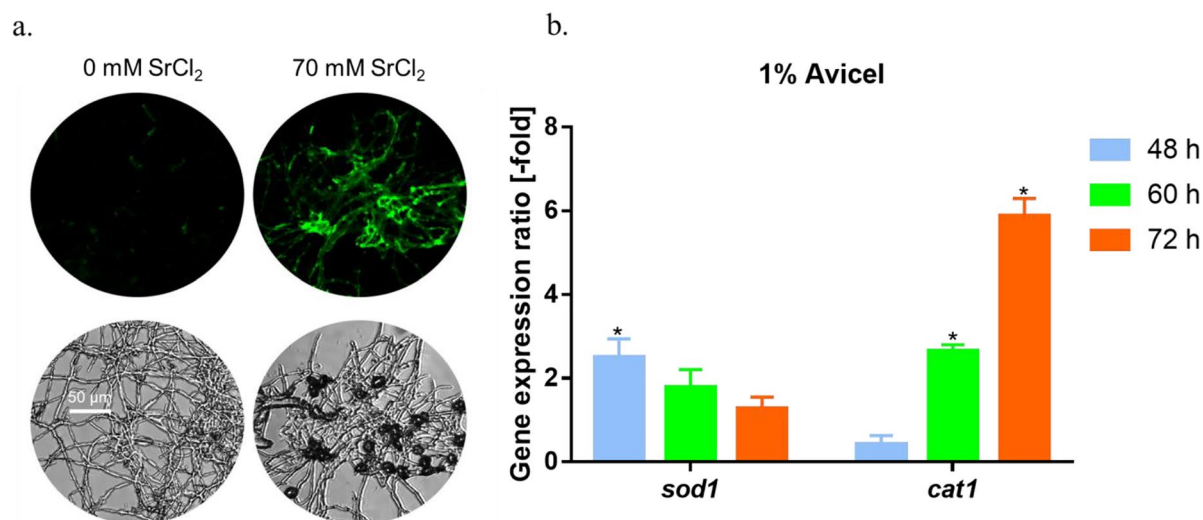

Fig. 6 Increase in cytosolic ROS level after Sr^{2+} addition. **a** Cytosolic ROS levels were detected using the specific fluorescent probe DCFH-DA. *Trichoderma reesei* RUT-C30 strain was cultured in liquid MM with $SrCl_2$ at a final concentration 0 or 70 mM for two days. To treat the hyphae, 10 μM DCFH-DA was used. The fluorescence intensity was monitored using automatic inverted fluorescence microscopy. Stronger green fluorescence indicated a higher intracellular ROS content. **b** Transcription levels of *sod1* and *cat1* were detected using RT-qPCR analysis, depicted as gene expression ratios [-fold] in RUT-C30 after treatment with 70 mM Sr^{2+} compared to RUT-C30 with no treatment on 1% Avicel for 48, 60, or 72 h. Gene expression ratios [-fold] were normalized to the corresponding gene expression at the same time point in the control (without Sr^{2+}). The final values are represented as the mean ± standard deviation (SD) of three independent experimental results. Asterisks indicate significant differences, representing gene expression ratios greater than twofold or less than 0.5-fold between the treated samples and those without Sr^{2+} treatment. DIC, differential interference contrast; RT-qPCR, reverse transcription quantitative polymerase chain reaction
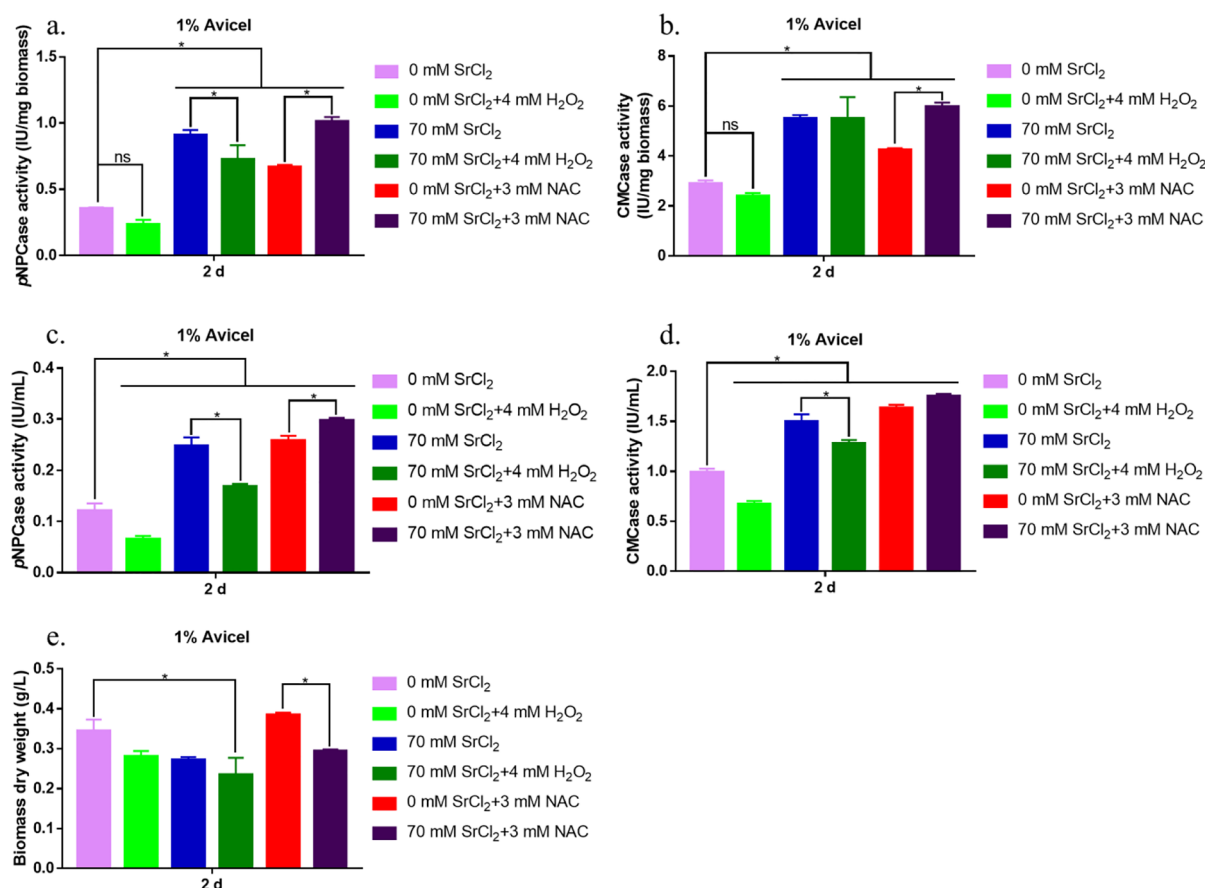
Li *et al. Bioresources and Bioprocessing*   (2022) 9:96

Page 9 of 12

Fig. 7 Effect of ROS on Sr^{2+}-induced cellulase production. *p*NPCase activity (**a** and **c**), CMCase activity (**b** and **d**), and biomass dry weight (**e**) were determined in the RUT-C30 strain after treatment with (or without) 70 mM Sr^{2+}, 4 mM H_2O_2, or 3 mM NAC in MM. The final values are represented as the mean ± standard deviation (SD) of three independent experimental results. Asterisks indicate significant differences compared to the strain without Sr^{2+} treatment ($p < 0.05$, according to Student's *t*-test). MM, minimal medium; ROS, reactive oxygen species

Discussion

Metal ions are essential for primary and secondary cellular metabolic processes. Ca^{2+} (Schmoll 2011) and Mg^{2+} (Blaszczyk and Duda-Chodak 2013) are critical environmental factors that affect primary and secondary metabolism in various organisms. There are few reports on the effects of Sr^{2+}, another group IIA metal ion. To the best of our knowledge, this study provides the first report that Sr^{2+} positively regulates cellulase production in *T. reesei* (Fig. 2a–e). Addition of 70 mM Sr^{2+} increased *p*NPCase and CMCase activity in the *T. reesei* wild-type strain QM6a by 53.3% and 51.6%, respectively, compared to those in the untreated control after 3 days of cultivation (Additional file 1: Figure S1a, b).

Addition of 70 mM Sr^{2+} had the most significant effect on cellulase activity. The upregulated expression levels of two major cellulase genes (*cbh1* and *egl1*) and the cellulase transcription factor (*ace3*) (Fig. 3) were consistent with the cellulase activity data. Overexpression of *ace3* enables a high level of cellulase production in *T. reesei* (Luo et al. 2020). This suggests that upregulated ACE3 may mediate Sr^{2+}-induced cellulase overexpression (Fig. 8). Addition of Sr^{2+} resulted in downregulation of *xyr1* expression (Fig. 3), suggesting that *xyr1* is not involved in this process.

Under Sr^{2+} pressure, treatment with Sr^{2+} led to a cytosolic Ca^{2+} burst and increased *crz1* transcription (Fig. 4c). According to previous studies, Ca^{2+} is an essential secondary messenger that can cooperate with intracellular cAMP (Benčina et al. 2005; Chen et al. 2021b), high-osmolarity glycerol (de Castro et al. 2014) and ROS (Chen et al. 2021a; Gao et al. 2018) to regulate life activities in filamentous fungi, which is worthy of further study. However, cytosolic Ca^{2+} burst (Fig. 4a, b) and cellulase overproduction (Fig. 5a–d) were eliminated by adding the plasma membrane Ca^{2+} channel blocker $LaCl_3$. These results indicate that calcium signal transduction is essential for Sr^{2+}-induced cellulase
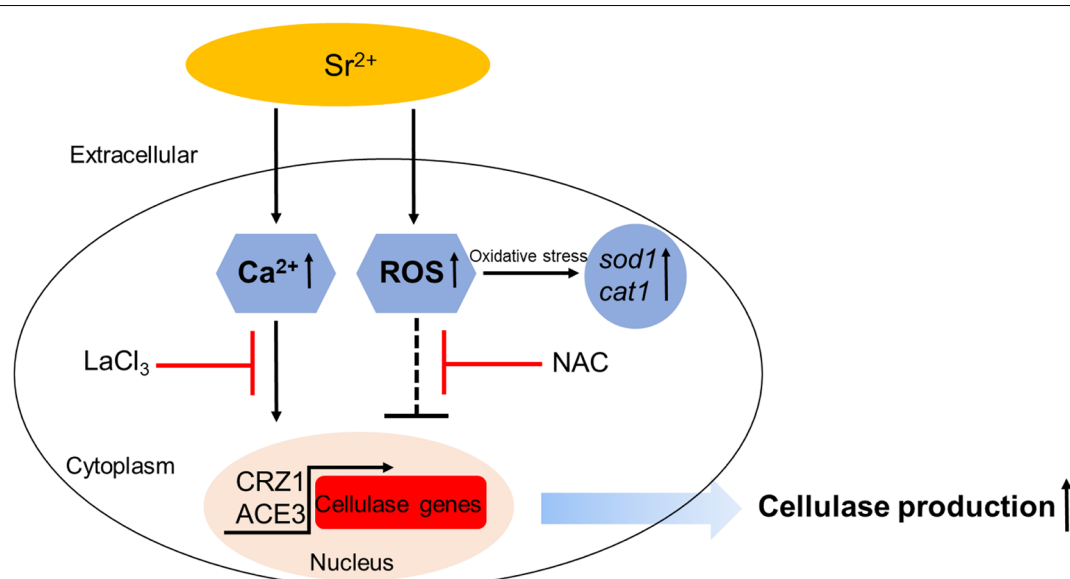
Fig. 8 Mechanistic model of Sr^{2+}-induced cellulase overexpression in *T. reesei*. Addition of 70 mM Sr^{2+} led to a significant increase in cytosolic Ca^{2+} levels, which in turn promoted overexpression of cellulase-related genes via Ca^{2+} signaling. The effect of adding NAC suggests that the cytosolic ROS burst induced by Sr^{2+} negatively affects cellulase secretion. Solid arrows indicate data supported by studies from our team, and dashed line indicate other undefined pathways. The red and black crosses represent repression. Black arrows indicate activation

production. This finding is similar to that of Chen et al. (2018), who reported that Mn^{2+} upregulates cellulase genes via calcium channels and signaling. Both Sr^{2+} and Mn^{2+} can induce cellulase overproduction; therefore, the process of Sr^{2+} induction is similar to that of the Mn^{2+}/Ca^{2+} transport system in cells. In *Thermosynechococcus elongatus*, Ca^{2+}/Sr^{2+} exchange affects photosystem II oxygen-evolving enzymes (Boussac et al. 2004) and electron transfer pathways from the S2 to S3 state (Boussac et al. 2015). Our results also demonstrate that Ca^{2+} plays a dominant role in Sr^{2+}-induced cellulase overproduction.

According to the periodic table of elements, the number of electrons in the outermost unpaired orbital of Sr^{2+} is the same as that of Ca^{2+}. This may partially explain their interaction and is worthy of further evaluated. Further studies are also required to investigate whether other metal ions interact with Ca^{2+} to regulate cellulase expression in *T. reesei*.

In this study, 70 mM Sr^{2+} inhibited growth of the strain (Fig. 1a–c), indicating that the strain was under pressure. Chen et al. (2016) reported that 100 mM Ca^{2+} repressed hyphal growth compared to that in the control. In addition, large amounts of ROS were produced after treatment with 70 mM Sr^{2+} based on analysis using an ROS probe (Fig. 6a). Gao et al. (2018) reported similar results, showing that treatment with Cu^{2+} significantly increased the intracellular ROS content in *G. lucidum*. Sr^{2+} was found to induce an increase in ROS levels, which affected

cellulase production and was eliminated by adding the ROS scavenger NAC (Fig. 7a–d). In *P. brevicompactum*, treatment with high concentrations of Ca^{2+} and Mn^{2+} results in a surge in ROS levels, which regulate the synthesis of the secondary metabolite mycophenolic acid (Chen et al. 2021a, 2022). In *G. lucidum*, ROS were previously found to induce overproduction of the secondary metabolite ganoderic acid (Liu et al. 2018). These results suggest that ROS acts as a signal to regulate cellulase expression in *T. reesei*; however, this prediction requires further study. NAC can relieve ROS pressure and improve cell growth and cellulase yield, and its supplementation can improve industrial enzyme production. Large amounts of renewable lignocellulose can be hydrolyzed into sugars by cellulase to produce biofuels and chemicals. Therefore, it is crucial to decrease the price of cellulase. In industrial cellulase production, supplementation with Sr^{2+} and an ROS scavenger can increase cellulase production and improve economic efficiency.

Conclusions

Our findings indicate that adding extracellular Sr^{2+} can rapidly and easily improve cellulase production. A putative mechanism was characterized to explain the effect of Sr^{2+} treatment on cellulase expression in *T. reesei* RUT-C30 (Fig. 8). When the strain was exposed to high concentrations of Sr^{2+} (70 mM), calcium signal transduction played a crucial role in Sr^{2+}-induced cellulase

Li *et al. Bioresources and Bioprocessing*　　(2022) 9:96

Page 11 of 12

production. However, the ROS content in the cytoplasm was significantly increased, thereby reducing cellulase expression. This study provides an effective approach for increasing cellulase production and insights into the effects of divalent metal ions on the life activities of filamentous fungi.

Abbreviations
CMCase: *Endo*-β-Glucanase activity; *crz1*: Calcineurin-responsive zinc finger transcription factor 1; FPase: Filter paper activity, representing total extracellular cellulase activity; *p*NPCase: Exo-β-glucanase activity; ROS: Reactive oxygen species; RT-qPCR: Real-time quantitative PCR.

Supplementary Information
The online version contains supplementary material available at https://doi.org/10.1186/s40643-022-00587-3.

> **Additional file 1: Figure S1.** Effects of Sr^{2+} on cellulase production in the parental strain QM6a. The *p*NPCase activity (a), CMCase activity (b) of *T. reesei* QM6a were measured after culture in MM medium for 2, 3, or 4 days with (or without) 70 mM Sr^{2+}. The final values are presented as the mean ± standard deviation (SD) of three independent experimental results. Asterisks indicate significant differences compared to the control ($p < 0.05$, according to Student's *t*-test).
>
> **Additional file 2: Table S1.** The primers used for RT-qPCR.

Declarations

Ethics approval and consent to participate
Not applicable.

Consent for publication
Not applicable.

Competing interests
The authors declare no competing interests.

References
Antoniêto AC, de Paula RG, Castro Ldos S, Silva-Rocha R, Persinoti GF, Silva RN (2016) *Trichoderma reesei* CRE1-mediated carbon catabolite repression in response to sophorose through RNA sequencing analysis. Curr Genomics 17(2):119–131

Baldrian P, Valásková V (2008) Degradation of cellulose by basidiomycetous fungi. FEMS Microbiol Rev 32(3):501–521

Benčina M, Legisa M, Read ND (2005) Cross-talk between cAMP and calcium signalling in *Aspergillus niger*. Mol Microbiol 56(1):268–281

Bischof R, Fourtis L, Limbeck A, Gamauf C, Seiboth B, Kubicek CP (2013) Comparative analysis of the *Trichoderma reesei* transcriptome during growth on the cellulase inducing substrates wheat straw and lactose. Biotechnol Biofuels 6(1):127

Blaszczyk U, Duda-Chodak A (2013) Magnesium: its role in nutrition and carcinogenesis. Rocz Panstw Zakl Hig 64(3):165–171

Bootman MD, Berridge MJ, Roderick HL (2002) Calcium signalling: more messengers, more channels, more complexity. Curr Biol 12(16):R563–R565

Boussac A, Rappaport F, Carrier P, Verbavatz J-M, Gobin R, Kirilovsky D, Rutherford AW, Sugiura M (2004) Biosynthetic Ca^{2+}/Sr^{2+} exchange in the photosystem II oxygen-evolving enzyme of *Thermosynechococcus elongatus*. J Biol Chem 279(22):22809–22819

Boussac A, Rutherford AW, Sugiura M (2015) Electron transfer pathways from the S_2-states to the S_3-states either after a Ca^{2+}/Sr^{2+} or a Cl^-/I^- exchange in Photosystem II from *Thermosynechococcus elongatus*. Biochim Biophys Acta 1847(6–7):576–586

Cao YL, Zheng FL, Zhang WX, Meng XF, Liu WF (2019) *Trichoderma reesei* XYR1 recruits SWI/SNF to facilitate cellulase gene expression. Mol Microbiol 112(4):1145–1162

Carle-Urioste JC, Escobar-Vera J, El-Gogary S, Henrique-Silva F, Torigoi E, Crivellaro O, Herrera-Estrella A, El-Dorry H (1997) Cellulase induction in *Trichoderma reesei* by cellulose requires its own basal expression. J Biol Chem 272(15):10169–10174

Chen L, Zou G, Wang JZ, Wang J, Liu R, Jiang YP, Zhao GP, Zhou ZH (2016) Characterization of the Ca^{2+}-responsive signaling pathway in regulating the expression and secretion of cellulases in *Trichoderma reesei* Rut-C30. Mol Microbiol 100(3):560–575

Chen YM, Shen YL, Wang W, Wei DZ (2018) Mn^{2+} modulates the expression of cellulase genes in *Trichoderma reesei* Rut-C30 via calcium signaling. Biotechnol Biofuels 11:54

Chen YM, Wu C, Shen YL, Ma YS, Wei DZ, Wang W (2019) *N, N*-dimethylformamide induces cellulase production in the filamentous fungus *Trichoderma reesei*. Biotechnol Biofuels 12:36

Chen MH, Wang JJ, Lin L, Xu XY, Wei W, Shen YL, Wei DZ (2021a) Synergistic regulation of metabolism by Ca^{2+}/reactive oxygen species in *Penicillium brevicompactum* improves production of mycophenolic acid and investigation of the Ca^{2+} channel. ACS Synth Biol 11(1):273–285

Chen YM, Fan XJ, Zhao XQ, Shen YL, Xu XY, Wei LJ, Wang W, Wei DZ (2021b) cAMP activates calcium signalling via phospholipase C to regulate cellulase production in the filamentous fungus *Trichoderma reesei*. Biotechnol Biofuels 14(1):62

Chen MH, Shen YL, Lin L, Wei W, Wei DZ (2022) Mn^{2+} modulates the production of mycophenolic acid in *Penicillium brevicompactum* NRRL864 via reactive oxygen species signaling and the investigation of pb-pho. Fungal Biol 126(6–7):461–470

de Castro PA, Chen CX, de Almeida RSC, Freitas FZ, Bertolini MC, Morais ER, Brown NA, Ramalho LNZ, Hagiwara D, Mitchell TK, Goldman GH (2014) ChIP-seq reveals a role for CrzA in the *Aspergillus fumigatus* high-osmolarity glycerol response (HOG) signalling pathway. Mol Microbiol 94(3):655–674

Fischer AJ, Maiyuran S, Yaver DS (2021) Industrial relevance of *Trichoderma reesei* as an enzyme producer. Methods Mol Biol 2234:23–43

Furukawa T, Shida Y, Kitagami N, Mori K, Kato M, Kobayashi T, Okada H, Ogasawara W, Morikawa Y (2009) Identification of specific binding sites for XYR1, a transcriptional activator of cellulolytic and xylanolytic genes in *Trichoderma reesei*. Fungal Genet Biol 46(8):564–574

Gao T, Shi L, Zhang TJ, Ren A, Jiang AL, Yu HS, Zhao MW (2018) Cross talk between calcium and reactive oxygen species regulates hyphal branching and ganoderic acid biosynthesis in *Ganoderma lucidum* under copper stress. Appl Environ Microbiol 84(13):e00438-18

Li *et al. Bioresources and Bioprocessing*   (2022) 9:96

Page 12 of 12

Groisman EA, Hollands K, Kriner MA, Lee E-J, Park S-Y, Pontes MH (2013) Bacterial Mg^{2+} homeostasis, transport, and virulence. Annu Rev Genet 47:625–646

Häkkinen M, Valkonen MJ, Westerholm-Parvinen A, Aro N, Arvas M, Vitikainen M, Penttilä M, Saloheimo M, Pakula TM (2014) Screening of candidate regulators for cellulase and hemicellulase production in *Trichoderma reesei* and identification of a factor essential for cellulase production. Biotechnol Biofuels 7(1):14

Li CC, Lin FM, Li YZ, Wei W, Wang HY, Qin L, Zhou ZH, Li BZ, Wu FG, Chen Z (2016) A β-glucosidase hyper-production *Trichoderma reesei* mutant reveals a potential role of cel3D in cellulase production. Microb Cell Fact 15(1):151

Li JG, Zhang SK, Li HL, Ouyang XH, Huang LL, Ni YH, Chen LH (2018) Cellulase pretreatment for enhancing cold caustic extraction-based separation of hemicelluloses and cellulose from cellulosic fibers. Bioresour Technol 251:1–6

Li YQ, Zhang YW, Zhang C, Wang HC, Wei XL, Chen PY, Lu L (2019) Mitochondrial dysfunctions trigger the calcium signaling-dependent fungal multidrug resistance. Proc Natl Acad Sci USA 117(3):1711–1721

Li YH, Yu JZ, Zhang P, Long TT, Mo Y, Li JH, Li Q (2021) Comparative transcriptome analysis of *Trichoderma reesei* reveals different gene regulatory networks induced by synthetic mixtures of glucose and β-disaccharide. Bioresour Bioprocess 8:57

Liu R, Cao PF, Ren A, Wang SL, Yang T, Zhu T, Shi L, Zhu J, Jiang AL, Zhao MW (2018) SA inhibits complex III activity to generate reactive oxygen species and thereby induces GA overproduction in *Ganoderma lucidum*. Redox Biol 16:388–400

Liu P, Zhang GX, Chen YM, Zhao J, Wang W, Wei DZ (2019) Enhanced cellulase production by decreasing intercellular pH through H^{+}-ATPase gene deletion in *Trichoderma reesei* RUT-C30. Biotechnol Biofuels 12:195

Livak KJ, Schmittgen TD (2001) Analysis of relative gene expression data using real-time quantitative PCR and the 2$^{-\Delta\Delta CT}$ Method. Methods 25(4):402–408

Luo Y, Valkonen M, Jackson RE, Palmer JM, Bhalla A, Nikolaev I, Saloheimo M, Ward M (2020) Modification of transcriptional factor ACE3 enhances protein production in *Trichoderma reesei* in the absence of cellulase gene inducer. Biotechnol Biofuels 13:137

Malagnac F, Lalucque H, Lepère G, Silar P (2004) Two NADPH oxidase isoforms are required for sexual reproduction and ascospore germination in the filamentous fungus *Podospora anserina*. Fungal Genet Biol 41(11):982–997

Martins-Santana L, de Paula RG, Silva AG, Lopes DCB, Silva RdN, Silva-Rocha R (2020) CRZ1 regulator and calcium cooperatively modulate holocellulases gene expression in *Trichoderma reesei* QM6a. Genet Mol Biol 43(2):e20190244

Martzy R, Mello-de-Sousa TM, Mach RL, Yaver D, Mach-Aigner AR (2021) The phenomenon of degeneration of industrial *Trichoderma reesei* strains. Biotechnol Biofuels 14(1):193

Mendoza-Martínez AE, Lara-Rojas F, Sánchez O, Aguirre J (2017) NapA mediates a redox regulation of the antioxidant response, carbon utilization and development in *Aspergillus nidulans*. Front Microbiol 8:516

Ren A, Liu R, Miao ZG, Zhang X, Cao PF, Chen TX, Li CY, Shi L, Jiang AL, Zhao MW (2017) Hydrogen-rich water regulates effects of ROS balance on morphology, growth and secondary metabolism via glutathione peroxidase in *Ganoderma lucidum*. Environ Microbiol 19(2):566–583

Roy A, Kumar A, Baruah D, Tamuli R (2021) Calcium signaling is involved in diverse cellular processes in fungi. Mycology 12(1):10–24

Schmoll M (2011) Assessing the relevance of light for fungi: implications and insights into the network of signal transmission. Adv Appl Microbiol 76:27–78

Somerville C, Youngs H, Taylor C, Davis SC, Long SP (2010) Feedstocks for lignocellulosic biofuels. Science 329(5993):790–792

Stricker AR, Grosstessner-Hain K, Würleitner E, Mach RL (2006) Xyr1 (xylanase regulator 1) regulates both the hydrolytic enzyme system and D-xylose metabolism in *Hypocrea jecorina*. Eukaryot Cell 5(12):2128–2137

Takemoto D, Tanaka A, Scott B (2007) NADPH oxidases in fungi: diverse roles of reactive oxygen species in fungal cellular differentiation. Fungal Genet Biol 44(11):1065–1076

Xin Q, Xu JT, Wang TH, Liu WF, Chen GJ (2010) Transcriptional regulation of cellulases and hemicellulases gene in *Hypocrea jecorina*—a review. Wei Sheng Wu Xue Bao 50(11):1431–1437

Yan S, Xu Y, Yu XW (2021) From induction to secretion: a complicated route for cellulase production in *Trichoderma reesei*. Bioresour Bioprocess 8:107

Zeilinger S, Mach RL, Schindler M, Herzog P, Kubicek CP (1996) Different inducibility of expression of the two xylanase genes xyn1 and xyn2 in *Trichoderma reesei*. J Biol Chem 271(41):25624–25629

Zhang GX, Liu P, Wei W, Wang XD, Wei DZ, Wang W (2016) A light-switchable bidirectional expression system in filamentous fungus *Trichoderma reesei*. J Biotechnol 240:85–93

Zhang JJ, Wu C, Wang W, Wang W, Wei DZ (2018) Construction of enhanced transcriptional activators for improving cellulase production in *Trichoderma reesei* RUT C30. Bioresour Bioprocess 5:40

Zhang JJ, Chen YM, Wu C, Liu P, Wang W, Wei DZ (2019) The transcription factor ACE3 controls cellulase activities and lactose metabolism via two additional regulators in the fungus *Trichoderma reesei*. J Biol Chem 294(48):18435–18450

Zhang XH, Ma C, Zhang L, Su M, Wang J, Zheng S, Zhang TG (2022) GR24-mediated enhancement of salt tolerance and roles of H$_2$O$_2$ and Ca^{2+} in regulating this enhancement in cucumber. J Plant Physiol 270:153640

Publisher's Note